Enhanced damage index method using torsion modes of structures

Seok Been Im[1], Harding C. Cloudt[2], Jeffrey A. Fogle[2] and Stefan Hurlebaus[*2]

[1]*ENG center, Samsung C&T, Seoul, Korea*
[2]*Zachry Department of Civil Engineering, Texas A&M University, College Station, USA.*

Abstract. A growing need has developed in the United States to obtain more specific knowledge on the structural integrity of infrastructure due to aging service lives, heavier and more frequent loading conditions, and durability issues. This need has spurred extensive research in the area of structural health monitoring over the past few decades. Several structural health monitoring techniques have been developed that are capable of locating damage in structures using modal strain energy of mode shapes. Typically in the past, bending strain energy has been used in these methods since it is a dominant vibrational mode in many structures and is easily measured. Additionally, there may be cases, such as pipes, shafts, or certain bridges, where structures exhibit significant torsional behavior as well. In this research, torsional strain energy is used to locate damage. The damage index method is used on two numerical models; a cantilevered steel pipe and a simply-supported steel plate girder bridge. Torsion damage indices are compared to bending damage indices to assess their effectiveness at locating damage. The torsion strain energy method is capable of accurately locating damage and providing additional valuable information to both of the structures' behaviors.

Keywords: damage index; bridge; structural health monitoring; pipe; torsion

1. Introduction

Infrastructure in the United States is beginning to age and surpass its design life. As time progresses, it is becoming more and more critical to be able to obtain a reliable approximation of the performance of certain transportation structures, namely bridges. Currently, bridge structures are being subjected to heavier loads at greater frequencies than initially anticipated partly due to an increase in the actual weight of vehicles and an increase in traffic. This overloading was not taken into consideration when initially designed. In addition, bridges may also be subjected to durability issues such as corrosion of structural or reinforcing steel, fatigue of steel members and components, or deterioration of concrete. Visual inspections are currently used to inspect bridges for these types of durability issues. These maintenance methods, however, are only performed on a scheduled basis, typically every other year, and they require trained personnel. Significant irreparable damage or even failure may be incurred over a two year period. Also, since these types of structures are very expensive and present a significant risk to human safety in the event of a

---

∗Corresponding author, Associate Professor, E-mail: shurlebaus@civil.tamu.edu

catastrophic collapse, precise quantifications of structural performance is valuable. For these reasons, there exists a demand for the ability to monitoring structural integrity on a continuous basis.

Several methods exist that are capable of locating and estimating damage based on the modal parameters of structure. Recently proven methods are time domain decomposition (TDD), frequency domain decomposition (FDD), and other decomposition methods. The three methods are used because they do not require the input or load applied to the structure when acquiring the modal parameters (Kim *et al*. 2005, Mizuno *et al*. 2008, Kim *et al*. 2010, Zhang *et al*. 2010).

Changes in natural or resonant frequencies are damage indicator that is commonly used. Cawley and Adams (1979) used changes in natural frequencies of a plate to accurately detect and locate damage and to roughly estimate the severity of damage. Their analysis became very computationally expensive. Conversely, Farrar *et al*. (1994) determined that frequency changes may not be accurate indicators of damage in some cases. Kim *et al*. (2003) compared the frequency-based damage detection method to a mode-shape based method and determined that both were capable of accurately locating damage for multiple damage scenarios. Kim's analysis also predicted false positives in addition to the accurate detections. Rytter and Kirkegaard (1997) applied the change in natural frequencies method to a full scale four story reinforced concrete building in order to detect damage and verified the results with visual inspections.

Pandey and Biswas (1994) present a method which locates damage based on changes in flexibility. Toksoy and Aktan (1994) successfully performed a verification of the change-in-flexibility method on a structural bridge to locate damage. Duffey *et al*. (2001) used axial modes to locate damage in a laboratory environment using axial strain energy and changes in flexibility. This verified that both methods were capable of detecting and locating damage. Lin (1998) used the unity check method in conjunction with the change-in-flexibility method to successfully detect damage. Topole (1997) mentions that there are some cases where using the change-in-flexibility method to detect damage is advantageous and there are others where it is disadvantageous.

Both, Doebling and Farrar (1997) and Stanbridge *et al*. (1997) have examined damage detection methods using direct changes in mode shapes. This method usually requires statistical analysis. Natke and Cempel (1997) applied the use of the change-in-mode-shape method to a finite element model of a cable-stayed bridge to successfully locate induced damage, and Ettouney *et al*. (1998) also applied this method in order to detect damage in a complex steel structure.

Pandey *et al*. (1991) presented a damage detection method that locates damage based on differences in modal bending curvature. The authors used the central difference method to numerically differentiate mode shapes and acquire mode shape curvatures. Their research did not take into account different types of structural behavior, though. Chance *et al*. (1994) found that the error incurred from numerically calculating mode shape curvature may be unacceptable.

Stubbs and Kim (1996) proposed a method for damage localization in structures using changes in modal parameters, particularly modal strain energy, from undamaged and damaged structures. This method is very general and can be applied to many different types of structures since it deals with modal strain energy using the modal stiffness of a certain mode shape. The experimental procedures of the paper used bending strain energy and did not consider other types of structural behavior. Similarly, Choi *et al*. (2006) proposed an advanced method for detecting damage in plate structures using modal strain energy; however, they also did not consider other types of structural behavior in their analyses. Park *et al*. (2001) validated the modal strain energy damage index method with measurements on a concrete box girder bridge and data from visual inspections. Ho

and Ewins (1999) found that unacceptable error may be incurred in using a strain energy damage index with bending curvatures; however, they analyzed modal curvature only. Also, other researchers have improved the damage index method to minimize error of raw data obtained from their field tests, but their approaches were limited to the modal curvature as well (Choi *et al.* 2008, You 2009, Huang *et al.* 2009).

Some practical problems exist with a bending curvature damage index method (DIM). Monitoring curvature directly requires the application of strain gages to the structure, which may be undesirable since installing strain gages may be difficult, tedious, expensive, and time consuming and could potentially cause detrimental effects such as corrosion or surface damage.

Usually, accelerations are measured, and necessary numerical derivatives are calculated to acquire the needed curvature for performing a DIM based on bending. Error is gained from formulating numerical derivates of raw data and, inevitably, data is lost. Error accumulated from unavoidable and inherent noise in signal processing combined with error introduced from numerical analysis may yield inaccurate and inconsistent damage indicating methods. Also, bending modes may not be a structure's most prominent modes of vibration since a structure may exhibit more pronounced torsion or axial modes of vibration. This could lead to a difficulty in measuring multiple bending mode shapes. Although Duffey *et al.* (2001) theoretically introduced the DIM using axial and torsional response in their research, their experiment was verified only for axial modes with a 9-DOF linear spring-mass system.

The torsional modes can be used for damage detection using the ordinary damage index method when the target structure is a plate-like structure such as a steel plate-girder bridge. Kim *et al.* (2007), Farrar and Jauregui (2001), and Samali *et al.* (2010) deal with torsional modes and also experimental verifications are already carried out to some extent.

For these reasons, an enhanced DIM is proposed in this paper which is based on modal torsion strain energy. Torsion strain energy is directly related to torsional rigidity and to the first derivative of the angle of twist. Twist of a structure can be easily ascertained through measurements, and less numerical approximations are needed to acquire further data, resulting in less error and a more accurate damage localization and estimation. However, most cases, where the damage identification methods were applied, have employed the bending responses of structures for localizing their damages. In structures such as pipes, shafts, and certain bridges, torsion mode shapes may be relevant to the total vibration of the structure. This research has verified the torsion-based DIM. Torsion based DIM will improve the current structural health monitoring approaches by providing a good indicator of damage in structures.

This paper is organized into two sections. The first section is an overview of the derivations of a new damage index method which is based on torsion strain energy and the mechanics of structural members. The second section reviews the numerical procedures performed to validate the theory described in the first section. It overviews the creation of two finite element models (FEM), data acquisition processes from the FEM, calculation processes, as well as a presentation and analysis of the final data. The second section includes case studies on a fixed-free pipe and a simply-supported steel girder bridge.

2. Damage index method based on torsion

Torsion strain energy, S_i, of the ith torsional mode shape can be described by

$$S_i = \int_0^L GJ(x)\left[\frac{d\theta_i(x)}{dx}\right]^2 dx \tag{1}$$

where L is the length of the structural member, $GJ(x)$ is the torsional rigidity, and θ_i is the modal relative angle of twist for the ith mode. Similarly, if a structural member is subdivided into n elements, the torsion strain energy of the ith mode and the nth element in a member is shown by

$$S_{in} = \int_a^b GJ_n\left[\frac{d\theta_i(x)}{dx}\right]^2 dx \tag{2}$$

where a and b are the starting and ending coordinates of the nth element, respectively, and GJ_n is the torsional rigidity in the nth element. Eqs. (1) and (2) are based on the undamaged conditions of the original structure. The modal strain energies based on torsion for damaged structures for both the entire member and each element are shown respectively by

$$S_i^d = \int_0^L GJ^d(x)\left[\frac{d\theta_i(x)}{dx}\right]^2 dx \tag{3}$$

and

$$S_{in}^d = \int_a^b GJ_n^d\left[\frac{d\theta_i^d(x)}{dx}\right]^2 dx \tag{4}$$

where the superscript d indicates parameters from a damaged structural element.

Similarly, the bending strain energy of the ith mode shape can be described by

$$S_i = \int_0^L EI(x)\left[\psi(x)\right]^2 dx \tag{5}$$

where $EI(x)$ is the bending stiffness and $\psi(x)$ is curvature and is the second derivative of displacement. Similar relationships to Eqs. (1), (2), (3) and (4) can be built based on bending strain energy. Using Eqs. (1) and (2), the fraction of strain energy in the ith mode can be built to give the fraction of total strain energy in the nth element and the ith mode by

$$F_{in} = \frac{S_{in}}{S_i} \tag{6}$$

Similarly using Eqs. (3) and (4) for the damaged case gives

$$F_{in}^d = \frac{S_{in}^d}{S_i^d} \tag{7}$$

and

$$\sum_{n=1}^N F_{in} = \sum_{n=1}^N F_{in}^d = 1 \tag{8}$$

For sufficiently large number of elements N, the fraction of strain energy in each element, F_{in} is very small. In addition, previous experiments showed that mode shapes having a damage were changed very little in undamaged locations (Mazurek and DeWolf 1990).

Assuming that the majority of the elements remain undamaged, since damage is usually a localized occurrence, the fraction of strain energy (F_{in}) remains relatively constant after a damage case (Stubbs and Kim 1996)

$$F_{in} \simeq F_{in}^d \tag{9}$$

Thus,

$$\frac{\int_a^b GJ_n \left[\frac{d\theta_i(x)}{dx} \right]^2 dx}{\int_0^l GJ(x) \left[\frac{d\theta_i(x)}{dx} \right]^2 dx} = \frac{\int_a^b GJ_n^d \left[\frac{d\theta_i^d(x)}{dx} \right]^2 dx}{\int_0^l GJ^d(x) \left[\frac{d\theta_i^d(x)}{dx} \right]^2 dx} \tag{10}$$

Assuming that $\int_0^l GJ(x)$ is approximately equal to $\int_0^l GJ^d(x)$, and the damage index for the nth element and the ith mode is obtained as follows

$$\beta_{in} = \frac{GJ}{GJ^d} = \frac{\int_a^b \left[\frac{d\theta_i^d(x)}{dx} \right]^2 dx \int_0^l \left[\frac{d\theta_i(x)}{dx} \right]^2 dx}{\int_0^l \left[\frac{d\theta_i^d(x)}{dx} \right]^2 dx \int_a^b \left[\frac{d\theta_i(x)}{dx} \right]^2 dx} \tag{11}$$

Finally, by summing the contributions to the damage index over all applicable modes, the damage index for the nth element becomes

$$\beta_n = \frac{\sum_{i=1}^{nm} f_{in}^d}{\sum_{i=1}^{nm} f_{in}} \tag{12}$$

where

$$f_{in} = \frac{\int_a^b \left[\frac{d\theta_i(x)}{dx} \right]^2 dx}{\int_0^L \left[\frac{d\theta_i(x)}{dx} \right]^2 dx} \tag{13}$$

and

$$f_{in}^d = \frac{\int_a^b \left[\frac{d\theta_i^d(x)}{dx} \right]^2 dx}{\int_0^L \left[\frac{d\theta_i^d(x)}{dx} \right]^2 dx} \qquad (14)$$

and *nm* is the number of modes collected. Similar relationships to Eqs. (13) and (14) may be built for the case of bending strain energy.

Stubbs and Kim (1996) developed a damage severity estimation by rearranging the terms in Eq. (9). Using the relationship that the damage index is equal to undamaged stiffness divided by the damaged stiffness and knowing that this relationship represents a scalar multiple of increased strain energy, this relation may be manipulated in order to calculate a fractional reduction in stiffness, i.e., a damage severity. The resulting equation for damage severity, α_n, in the *n*th element becomes

$$\alpha_n = \frac{1}{\beta_n} - 1 \qquad (15)$$

Damage is incurred in an element when α_n is less than zero. If α_n is greater than or equal to zero, then no damage is predicted in the element under investigation.

Kim and Stubbs (2002) introduced the following damage index

$$z_n = \frac{\beta_n - \mu_\beta}{\sigma_\beta} \qquad (16)$$

where z_n is a normalized damage index for each *n*th element, μ_β *is* the average of the damage indices for the entire member, and σ_β is the standard deviation of the damage indices for the entire member. The normalized damage index is particularly useful since it pronounces the deviations from the mean damage index which improves localization of damage, and decreases the amount of false positive damage predictions.

3. Case studies

3.1 Finite element model and data acquisition

A numerical procedure was developed to test the proposed torsion damage index method. The procedure was carried out using two separate finite element models (FEM) which will be discussed later.

The software package used is equipped with an approximate modal analysis function that uses the eigenvector method and is given by

$$\left[\mathbf{K} - \Omega_i^2 \mathbf{M} \right] \phi = 0 \qquad (17)$$

where $\mathbf{K}$ is the system stiffness matrix, Ω_i is the eigenvalue of a *i*th mode shape, $\mathbf{M}$ is the system mass matrix, and ϕ is the particular mode shape vector associated with a particular eigenvalue.

Eq. (16) is solved numerically for a user-defined quantity of modes by using an accelerated sub-space iteration algorithm. When a specified tolerance between iterations is reached, an eigenvalue and corresponding eigenvector are found. This process is continued until all of the predefined modes have been found.
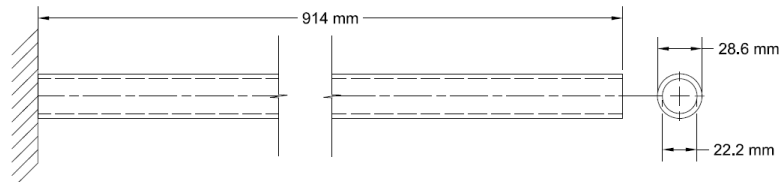
Fig. 1 Dimensions of cantilever pipe

3.2 Example I: pipe

Fig. 1 shows a drawing of a model used to collect mode shapes for testing the proposed damage index method. The FEM was created using shell elements capable of modeling both plate bending and plate stretching degrees of freedom. The shown model represents the undamaged, pristine condition of the pipe. The pipe is characterized by an overall length of 914.4 mm, a mean diameter of 25.4 mm, and a wall thickness of 3.175 mm. The boundary conditions used are a fixed condition at one end of the pipe and a free condition at the other end. The material used is that of conventional steel with Young's modulus of 200 GPa and Poisson's ratio of 0.3.

In order to acquire damaged mode shapes, a damaged FEM is developed. Damage is induced into the FEM by applying different material properties. For the purposes of this research, the Young's modulus for steel, and subsequently the shear modulus, was modified in a ring of shell elements at midspan to contain a 25% reduction.

Mode shapes were collected from each FEM. The mode shapes collected for this research were the first three bending mode shapes and the first three twisting or torsion mode shapes. The first three collected bending and torsion modes shapes are shown in Fig. 2.
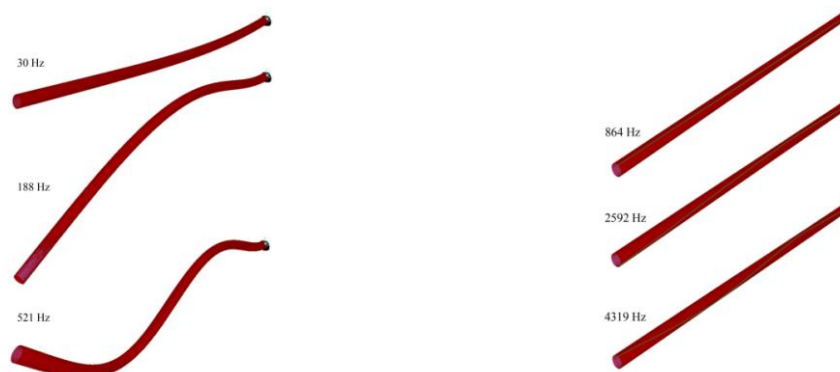
Fig. 2 Bending mode shapes (left) and torsion mode shapes (right)

Using the mechanics relationships and damage index equations, values for the damage index of each successive pipe element are created. The normalized torsion and bending damage indices, z_j, are shown in Fig. 3 and the torsion and bending damage severities, α_j, are shown in Fig. 4.
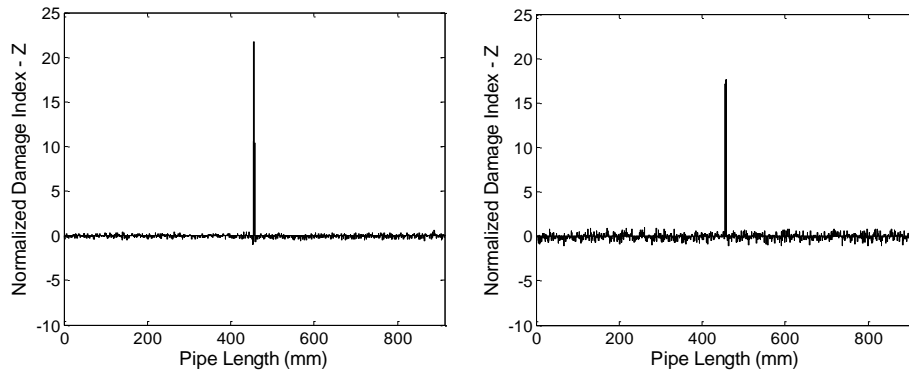

Fig. 3 Bending damage index with 3% noise (left) and torsion damage index with 3% noise (right)
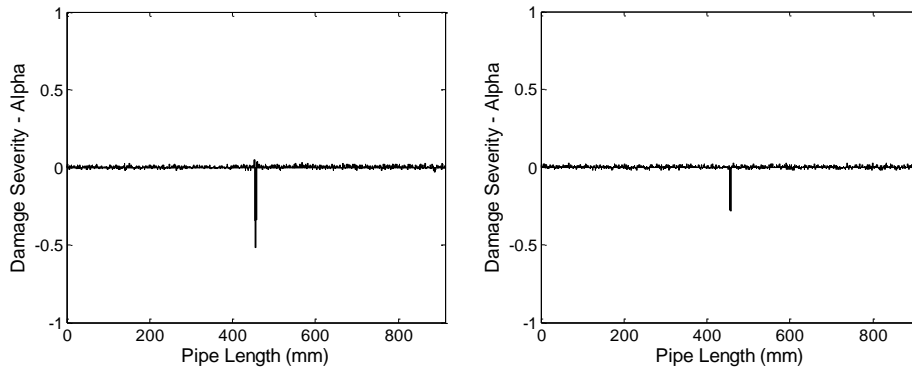

Fig. 4 Bending damage severity with 3% noise (left) and torsion damage severity with 3% noise (right)

After considering 3% white noise ($\mu=0$, $\sigma^2=1$) in the numerical analysis, the damage index calculations using both bending mode shapes and torsion modes shapes are capable of locating damage. Without noise, however, small deviations are exhibited near peak points when using the bending damage index. These deviations occur because of the nature of the data collected. When using bending mode shapes, numerical differentiation is necessary since the collected data is modal displacement, but modal curvature is required. In order to acquire modal curvature, two derivatives of the modal displacement must be taken. The bending damage index requires two derivates and locates damage in three adjacent elements according to Fig. 3, and the torsion damage index requires one derivative and locates damage in two elements according to Fig. 3, where in simulation there is damage in only one element. This logically implies that as more numerical differentiations are performed, the damage index method becomes less capable of accurately locating damage. Also, the numerical analysis of the raw data creates some spillover

effect in the damage indices taken from bending mode shapes as can be seen from Fig. 3. The effect is that of broadening the location of detected damage, heightening the severity of detected damage, and detecting a stiffness increase in closely neighboring elements.

Also, it can be seen from Fig. 4 that the torsion damage severity estimates damage more accurately in this case. A detected damage severity of 27.6% with the torsion modes compares well with simulated damage severity of 25% in comparison to the detected damage severity of 43.2% with bending modes.

3.3 Example 2: bridge

The torsion damage index method is performed on a FEM of a built-up steel plate girder rail bridge. A picture of the FEM is shown in Fig. 5. The bridge has a 19.8 m span and has intermittent cross braces and shear stiffeners for stability. The bridge also has a 0.457 m flange width, an overall depth of 1.69 m, and 1.98 m spacing between girders. The boundary conditions of the FEM are simply-supported.
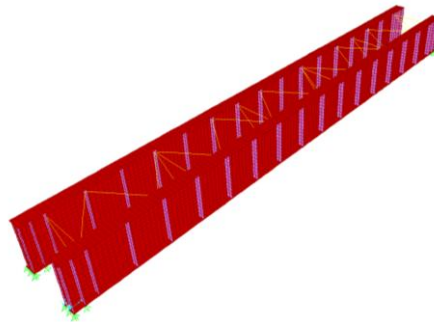

Fig. 5 FEM of Bridge

Table 1 Natural frequencies of the bridge model before and after damage

Mode No.	Natural frequency before damage (Hz)	Natural frequency after damage (Hz)	Note
1	10.24	10.25	1st lateral bending mode
2	17.79	17.81	1st torsion mode
3	18.15	18.18	1st vertical bending mode
4	21.78	20.97	2nd lateral bending mode
5	35.19	35.23	3rd lateral bending mode
6	40.79	40.79	2nd torsion mode
7	46.05	46.05	2nd vertical bending mode

In order to induce damage to this bridge, one of the bracing elements is simply removed. In this study, a bracing element that connects the top flange of one girder to the top flange of the adjacent girder is removed. The locations of the connections for this brace are at a 10.5 m length of the

right-most girder and a 9.30 m length of the left-most girder in Fig. 5. As can be expected, removing bracing elements affects the vibration properties of the vertical, in-plane bending mode shapes less than the torsional and horizontal bending mode shapes since the braces are used for lateral stability. For this reason, lateral, out-of-plane bending mode shapes are collected from this structure, as well as torsion mode shapes, because of the effect that the removal has on the lateral bending and torsion resistance. The natural frequencies of the structure before and after damage are provided in the Table 1.

Displacements and rotations are collected from this structure at the center of the top flange of the right-most girder at each joint along the length of the bridge. Three lateral bending mode shapes, two vertical bending mode shapes, and two torsion mode shapes are collected. The lateral bending, vertical bending, and torsion mode shapes are shown in Figs. 6, 7 and 8, respectively.
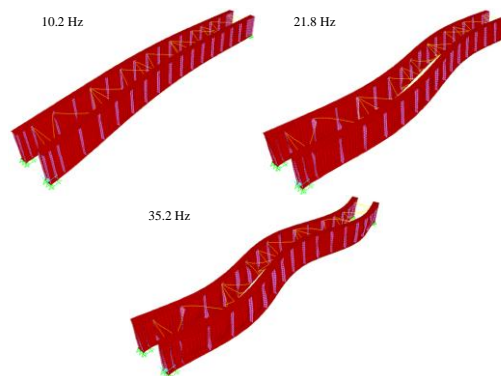
Fig. 6 First lateral bending mode (top left), second lateral bending mode (top right), and third lateral bending mode (bottom)
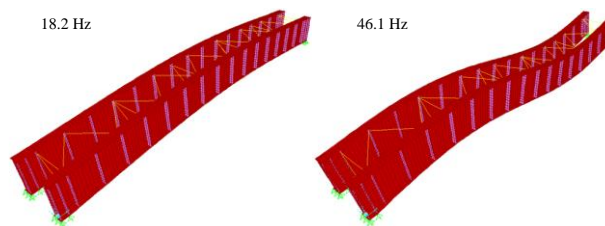
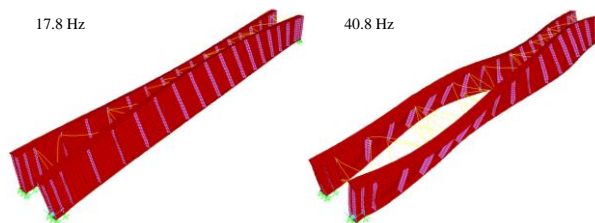Fig. 7 First vertical bending mode (left) and second vertical bending mode (right)

Fig. 8 First torsion mode (left) and second torsion mode (right)

The damage indices for lateral bending, vertical bending, and torsion are shown in Figs. 9, 10, and 11 respectively. The 3% white noise ($\mu=0$, $\sigma^2=1$) is considered in the numerical data. Because the noise may lead to a false alarm in each damage index, the damage indices in Figs. 9, 10 and 11 are obtained using an average index of 10 data sets. As can be seen from the figures, the lateral bending damage index of Fig. 9 predicts damage in several elements but two general locations, the vertical bending damage index of Fig. 10 detects damage in multiple elements over the entire length of the bridge, and the torsion damage index of Fig. 11 predicts damage in multiple elements but one most significant location. Since the lateral bending damage index detects damage in two general areas, this leads to the assumption that when damage is induced in the bridge by removing bracing elements, the load path through the bracing elements is changed for lateral bending, and elements adjacent to the removed element must pick up the forces it would have carried. The vertical bending damage index detects damage in elements throughout the length of the beam and not in one localized area. This confirms the assumption that vertical bending modes do not provide much information for the detection of damage by removal of a diaphragm element. The torsion damage index, however, correctly identifies the one most significant location of damage at the connection of the removed brace on the right-most girder's top flange at a length of 10.5 m. The information provided by the torsion damage index in this case is useful for eliminating one of the two damage detections in the lateral bending damage index where a brace is not removed on the flange where data is collected.
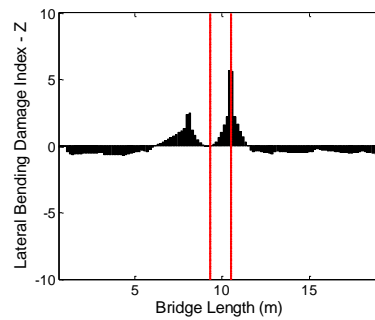

Fig. 9 Lateral bending damage index of bridge with 3% noise (space between vertical lines indicates location of actual damage)
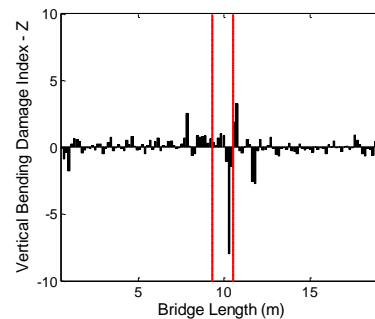

Fig. 10 Vertical bending damage index of bridge with 3% noise (space between vertical lines indicates location of actual damage)
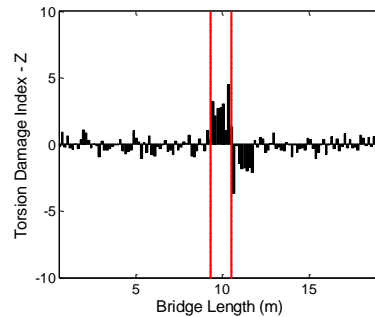
Fig. 11 Torsion damage index of bridge with 3% noise (space between vertical lines indicates location of actual damage)

The number of data collected from the sensors in the field is limited as a realistic application. Thus, sparsely arranged 21 data points (spacing 0.91 m) are selected from the numerical results and each data are polluted by 3% white noise. To provide better torsion mode shapes from the limited data, the cubic spline interpolation technique is used. The noise effect is minimized using an average damage index from ten data sets. Fig. 12 exhibits the torsion damage index using sparsely arranged data with noise polluted. It is able to locate the damage location in the bridge model.
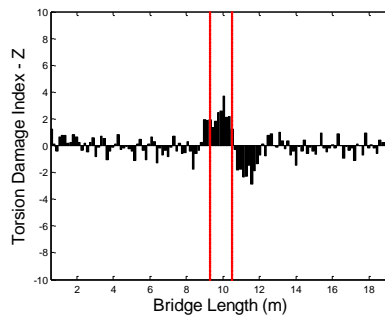

Fig. 12 Torsion damage index of bridge using sparsely arranged data with 3% noise (space between vertical lines indicates location of actual damage).

4. Conclusions

The torsion damage index is first derived, and then it is applied to two separate case studies. First, a numerical analysis was performed on a FEM of a pipe. The second analysis was performed on a FEM of a bridge structure. The torsion damage index was successful at locating damage in both structures. The torsion damage index compared very well with the bending damage index, and, in some scenarios, torsion damage more accurately locates damage than the bending damage index. Also, the torsion damage index method using sparsely arranged data which are polluted by noise is capable of identifying the damage location where a brace is removed. The findings

indicate that there are cases where torsion modes may be desirable to collect providing additional information of the structural integrity. These cases are likely limited to structures which exhibit torsional behavior.

Acknowledgements

References

Cawley, P. and Adams, R.D. (1979), "The location of defects in structures from measurement of natural frequencies". *J. Strain Anal. Eng.*, **14**(2), 49-57.

Chance, J., Tomlinson, G.R. and Worden, K. (1994), "A simplified approach to the numerical and experimental modeling of the dynamics of a cracked beam", *Proceedings of the SPIE 12th International Modal Analysis Conference.*

Choi, F., Li, J., Samali, B. and Crews, K. (2008), "Application of the modified damage index method to timber beams", *Eng. Struct.*, **30**, 1124-1145

Choi, S., Park, S., Park, N.H. and Stubbs, N. "Improved fault quantification for a plate structure", *J. Sound Vib.*, **297**, 865-879.

Doebling, S.W. and Farrar, C.R. (1997), "Using statistical analysis to enhance modal-based damage identification", *Proceedings of the DAMAS '97 Structural Damage Assessment Using Advanced Signal Processing*, University of Sheffield, UK.

Duffey, T.A., Doebling, S.W., Farrar, C.R., Baker, W.E. and Rhee, W.H. (2001), "Vibration-based damage identification in structures exhibiting axial and torsional response", *J. Vib. Acoust.*, **123**, 84-91.

Ettouney, M., Daddazio, R., Hapij, A. and Aly, A. (1998), "Health monitoring of complex structures", *Proceedings of the SPIE Smart Structures and Materials 1998: Industrial and Commercial Applications of Smart Structures Technologies.*

Farrar, C.R. and Jauregui, D. (2001) *Damage detection algorithms applied to experimental and numerical modal data from the 1-40 bridge*, LA-13074-MS, Report of Los Alamos National Laboratory.

Farrar, C.R., Baker, W.E., Bell, T.M., Cone, K.M., Darling, T.W., Duffey, T.A., Eklund, A. and Migliori, A. (1994), *Dynamic characterization and damage detection in the I-40 bridge over the Rio Grande*, Los Alamos National Laboratory Report LA-12767-MS, Los Alamos National Laboratory, Los Alamos.

Ho, Y.K. and Ewins, D.J. (1999), "Numerical evaluation of the damage index", *Proceedings of the 2nd International Workshop on Structural Health Monitoring,* Stanford University, Palo Alto, California.

Huang, Q., Gardoni, P. and Hurlebaus, S. (2009), "Probabilistic capacity models and fragility estimates for reinforced concrete columns incorporating NDT data", *J. Eng. Mech. - ASCE*, **135**(12), 1384-1392.

Kim, B., Stubbs, N. and Park, T. (2005), "A new method to extract modal parameters using output-only responses", *J. Sound Vib.*, **282**, 215-230.

Kim, B., Lee, J. and Lee, D.H. (2010), "Extracting modal parameters of high-speed railway bridge using the TDD technique", *Mech. Syst. Signal Pr.*, **3**, 707-720.

Kim, J.T., Park, J.H. and Lee, B.J. (2007). "Vibration-based damage monitoring in model plategirder bridges under uncertain temperature conditions", *Eng. Struct.*, **29**(7), 1354-1365

Kim, J.T. and Stubbs, N. (2002), "Improved damage identification method based on modal information", *J. Sound Vib.*, **252**, 223-238.

Kim, J.T., Ryu, Y.S., Cho, H.M. and Stubbs, N. (2003), "Damage identification in beam-type structures: frequency-based method vs. mode-shape-based method", *Eng. Struct.*, **25**, 57-67.

Lin, C. (1998), "Unity check method for structural damage detection", *J. Spacecraft Rockets*, **35**(4), 577-579.

Mazurek, D.F. and DeWolf, J.T. (1990), "Experimental study of bridge monitoring technique", *J. Struct. Eng. - ASCE*, **116**(9), 2532-2549.

Mizuno, Y., Monroig, E. and Fujino, Y. (2008), "Wavelet decomposition-based approach for fast damage detection of civil structures", *J. Infrastruct. Syst.*, **14**(1), 27-32.

Natke, H.G. and Cempel, C. (1997), "Model-aided diagnosis based on symptoms", *Proceedings of the DAMAS '97, Structural Damage Assessment Using Advanced Signal Processing Procedures*, University of Sheffield, UK, 363-375.

Pandey, A.K. and Biswas, M. (1994), "Damage detection in structures using changes in flexibility", *J. Sound Vib.*, **169**(1), 3-17.

Pandey, A.K., Biswas, M. and Samman, M.M. (1991), "Damage detection from changes in curvature mode shapes", *J. Sound Vib.*, **145**(2), 321-332.

Park, S., Stubbs, N., Bolton, R. and Choi, S. (2001), "Field verification of the damage index method in a concrete box-girder bridge via visual inspection", *Comput. Aided Civil. Infrastruct. Eng.*, **16**, 58-70.

Rytter, A. and Kirkegaard, P. (1997), "Vibration based inspection using neural networks", *Proceedings of the DAMAS '97, Structural Damage Assessment Using Advanced Signal Processing*, University of Sheffield, UK, 97-108.

Samali, B., Li, J., Choi, F.C. and Crews., K. (2010). "Application of the damage index method for plate-like structures to timber bridges", *Struct. Health Monit.*, **17(8)**, 849-871.

Stanbridge, A.B., Khan, A.Z. and Ewins, D.J. (1997), *Fault quantification in vibrating structures using a scanning laser doppler vibrometer, Structural Health Monitoring, Current Status and Perspectives*, Stanford University, Palo Alto, California.

Stubbs, N. and Kim, J.T. (1996), "Damage localization in structures without baseline modal parameters", *AIAA J.* **34**(8), 1644-1649.

Toksoy, T. and Aktan, A.E. (1994), "Bridge-condition assessment by modal flexibility", *Exp. Mech.*, **34**, 271-278.

Topole, K. (1997), "Damage evaluation via flexibility formulation", *Proceedings of the SPIE* 3043*Smart Systems for Bridges, Structures, and Highways*, May.

You, T. (2009), *Iterative damage index method for structural health monitoring*, Master Thesis, Texas A&M University, College Station, Texas, USA.

Zhang, L., Wang, T. and Tamura, Y. (2010), "A frequency-spatial domain decomposition (FSDD) method for operational modal analysis", *Mech. Syst. Signal Pr.*, **24**(5), 1127-1239.